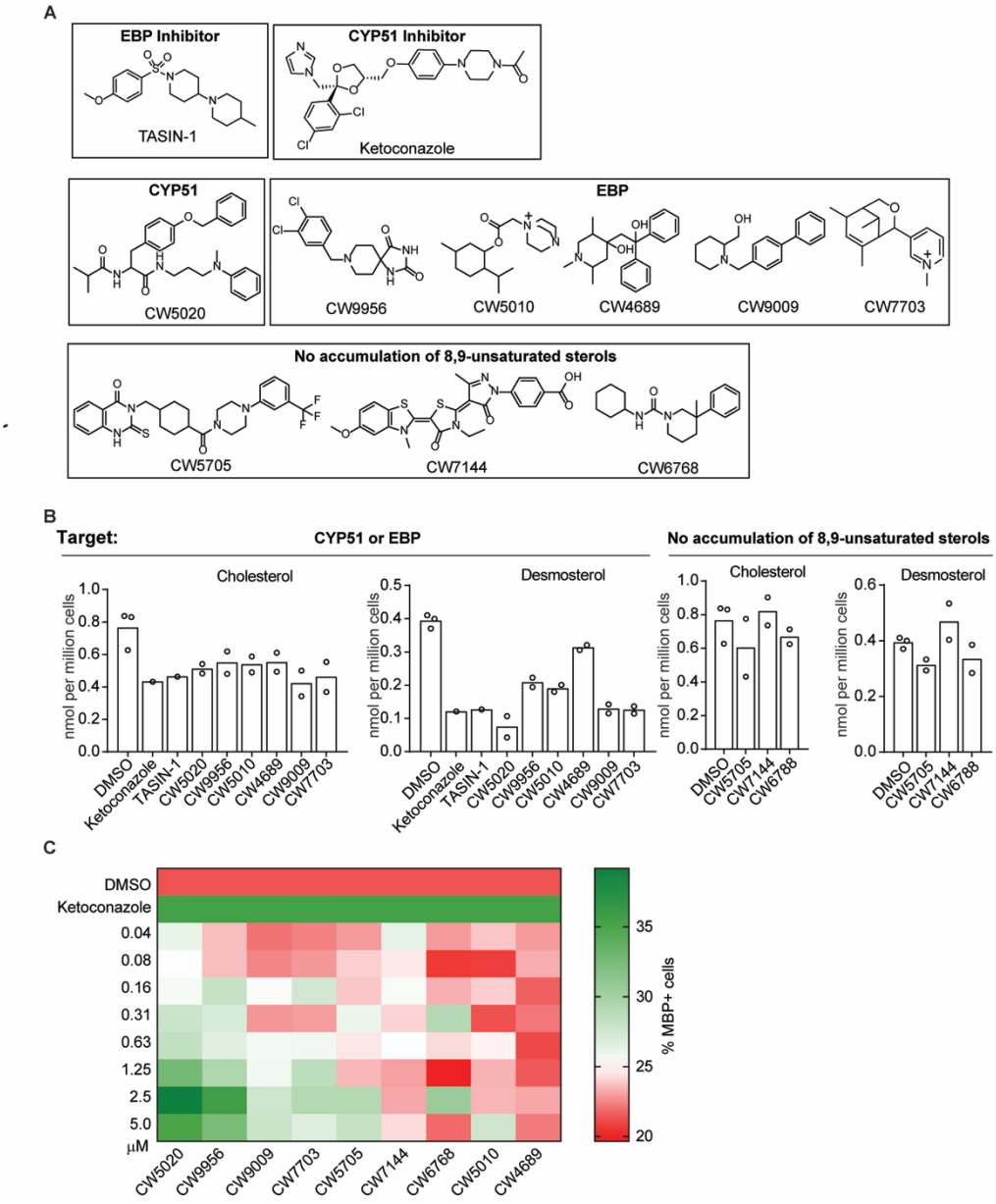

Figure S1. Validation of top high-throughput screen hits in two independent derivations of OPCs (OPC-1 and OPC-5) and their effects on cholesterol biosynthesis in OPCs. Related to Figure 1. A. Structure of top HTS-hits and known selective inhibitors of CYP51 and EBP. B. GC-MS-based quantification of cholesterol and desmosterol in OPCs after treatment with indicated small molecules at 10 μM. C. Heatmap representing the dose-dependent effects of HTS hits on MBP+ oligodendrocyte formation from OPC-5 cells after 72 h. Dose-response begins at 5 μM, whereas original screen tested all molecules at 10 μM.

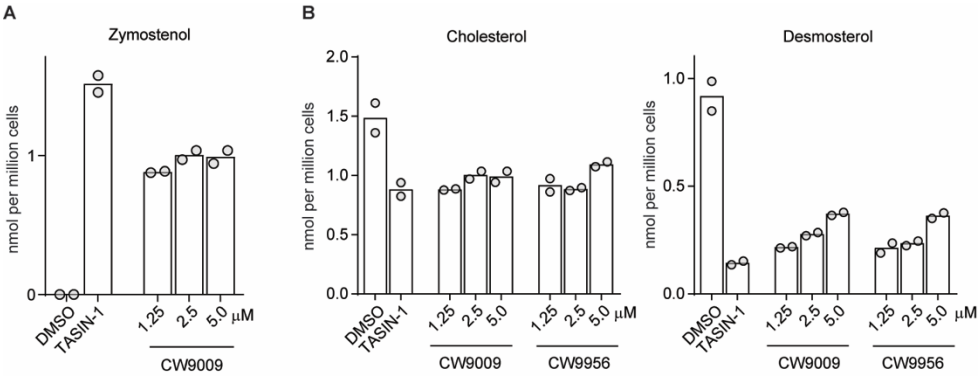

Figure S2 . Effect of CW9009 or CW9956 treatment on sterol levels in OPCs. Related to Figure 2. A. GC-MS-based quantification of zymostenol in OPC-5 cells after treatment with CW9009. B. Quantification of cholesterol and desmosterol in OPC-5 after treatment with CW9009 or CW9956 at indicated concentrations.

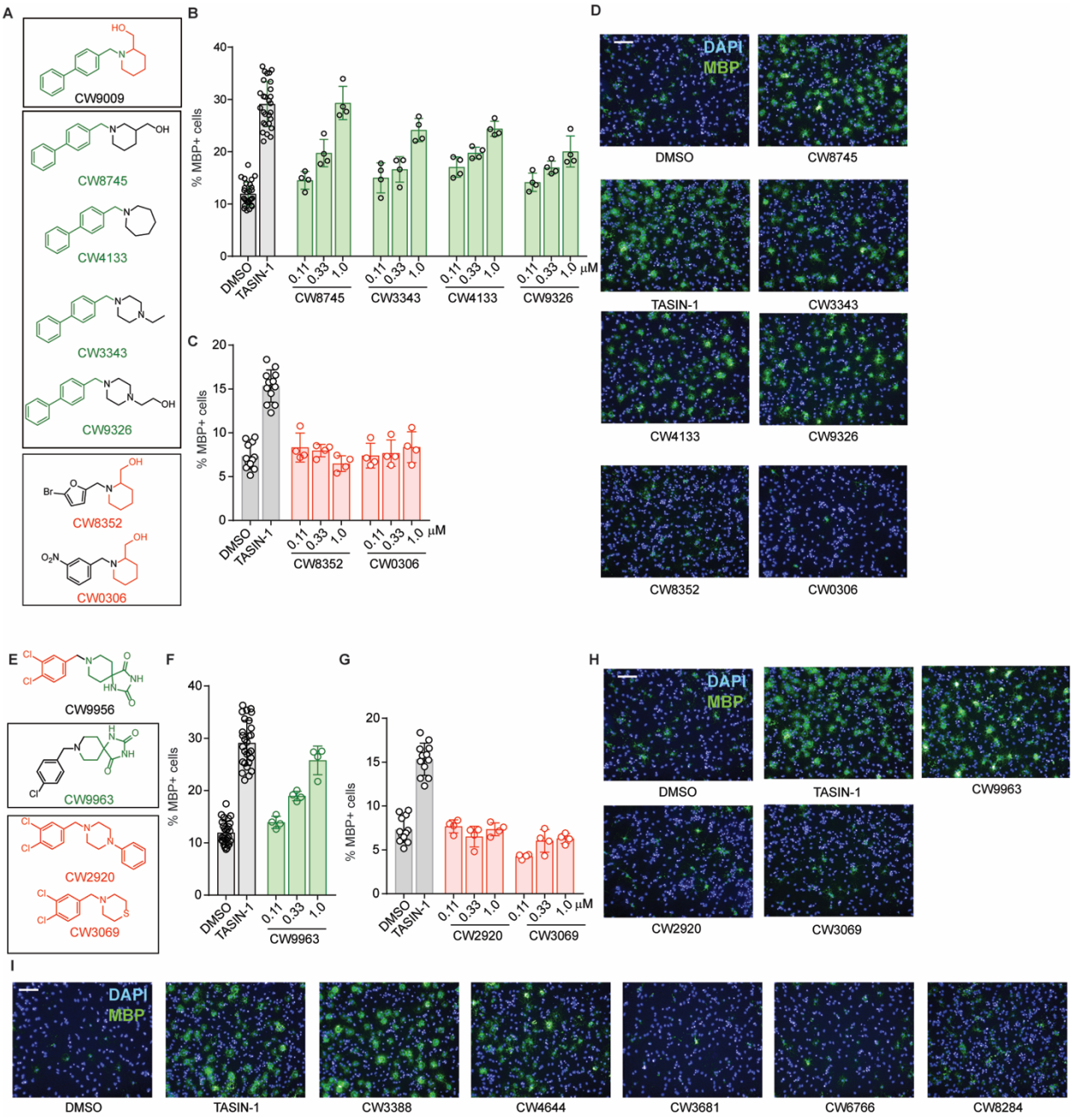

Figure S3. Structure activity relationship analysis on analogs of CW9009 reveals the biaryl moiety as important for enhancing oligodendrocyte formation. Related to Figure 3. A. Structure of analogs of CW9009, with biaryl functionality colored green. B,C. Percentage of MBP+ oligodendrocytes generated in OPC-5 after treatment with the indicated concentrations of small molecules for 72 h. D. Representative images of OPCs treated with DMSO or the indicated molecules at 1 μM. Green labels indicate molecules that enhance oligodendrocyte formation, while red labels indicate molecules with no effect on oligodendrocyte formation. E. Structure of analogs of CW9956. F, G. Percentage of MBP+ oligodendrocyte generated in OPC-5 after treatment with indicated small molecules at given concentrations for 72 h. H. Representative images of OPCs

treated with DMSO or indicated molecules at 1 μM. I. Representative images of OPCs treated with molecules presented in Figure 3. Green labels indicate molecules enhancing oligodendrocyte formation, while red labels indicate molecules with no effect on oligodendrocyte formation. Error bars represent standard deviation.

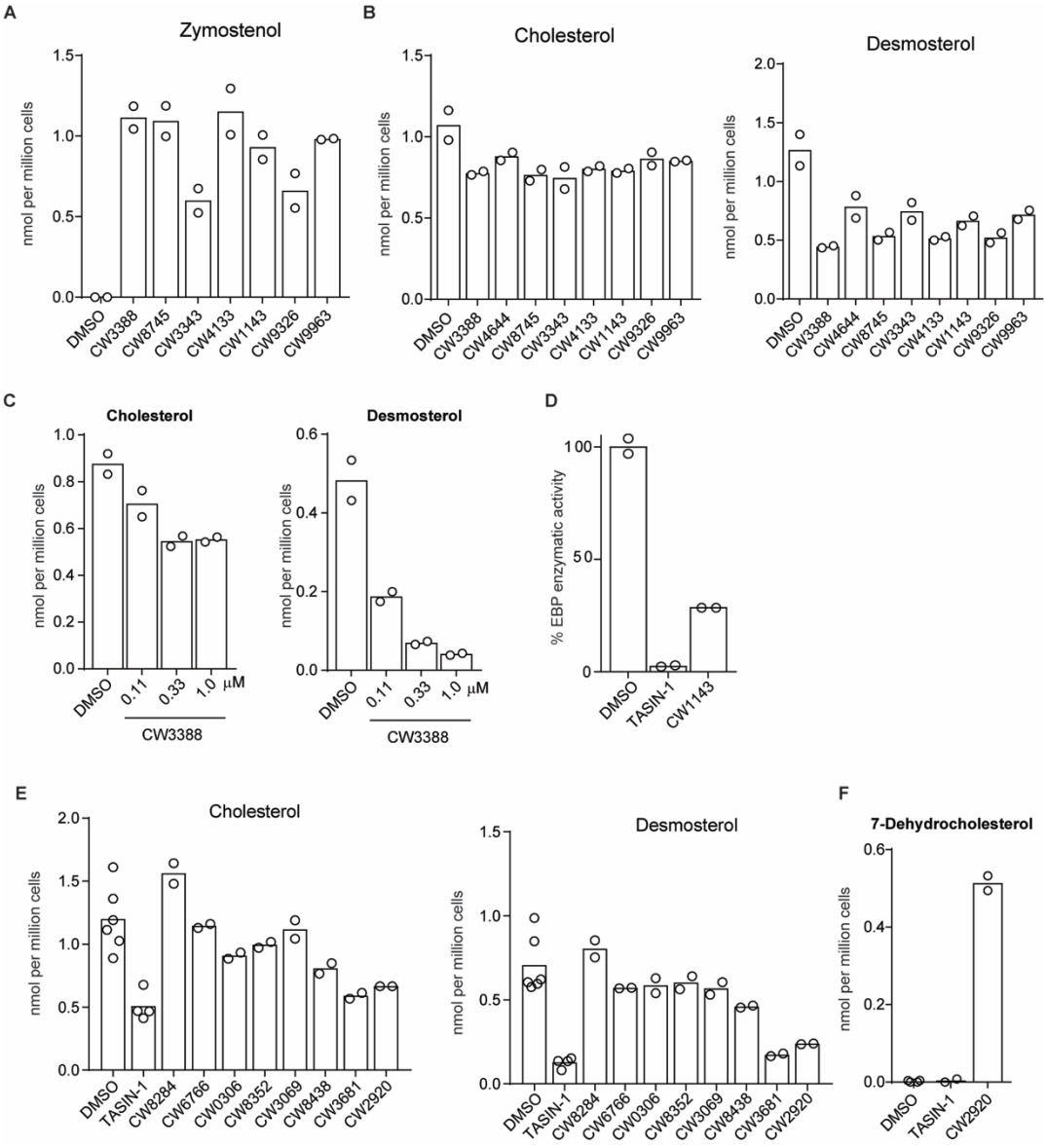

Figure S4. GC-MS-based sterol profiling in OPC-5 after treatment with structural analogs of CW9009/CW9956. Related to Figure 3. A, B. Quantification of zymostenol (A) or cholesterol and desmosterol (B) in OPCs after treatment with small molecule enhancers of oligodendrocyte formation. C. Levels of cholesterol and desmosterol measured in OPCs after treatment with CW3388 (at indicated doses) using GC-MS. D. EBP enzymatic activity in a biochemical assay at 10 μM. E, Quantification of cholesterol and desmosterol using GC-MS in OPCs after treatment with small molecules that showed no effect on oligodendrocyte formation. F. GC-MS-based quantification of 7-dehydrocholesterol in CW2920-treated OPCs. In A, B, E, and F, all treatment concentrations were at 1 μM.

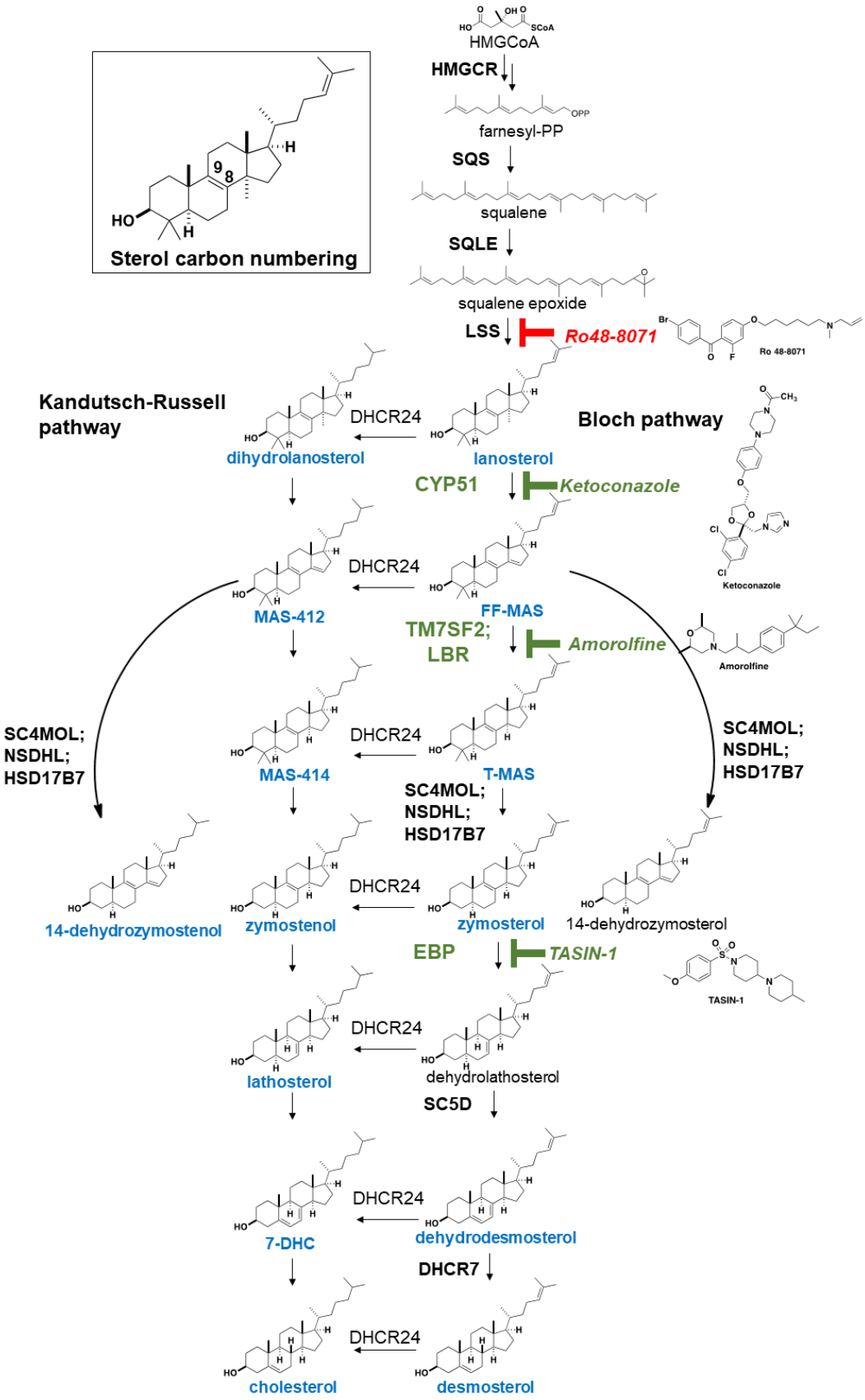

Data S1: Cholesterol biosynthesis pathway intermediates. Adapted from reference 6. Related to Figure 2.

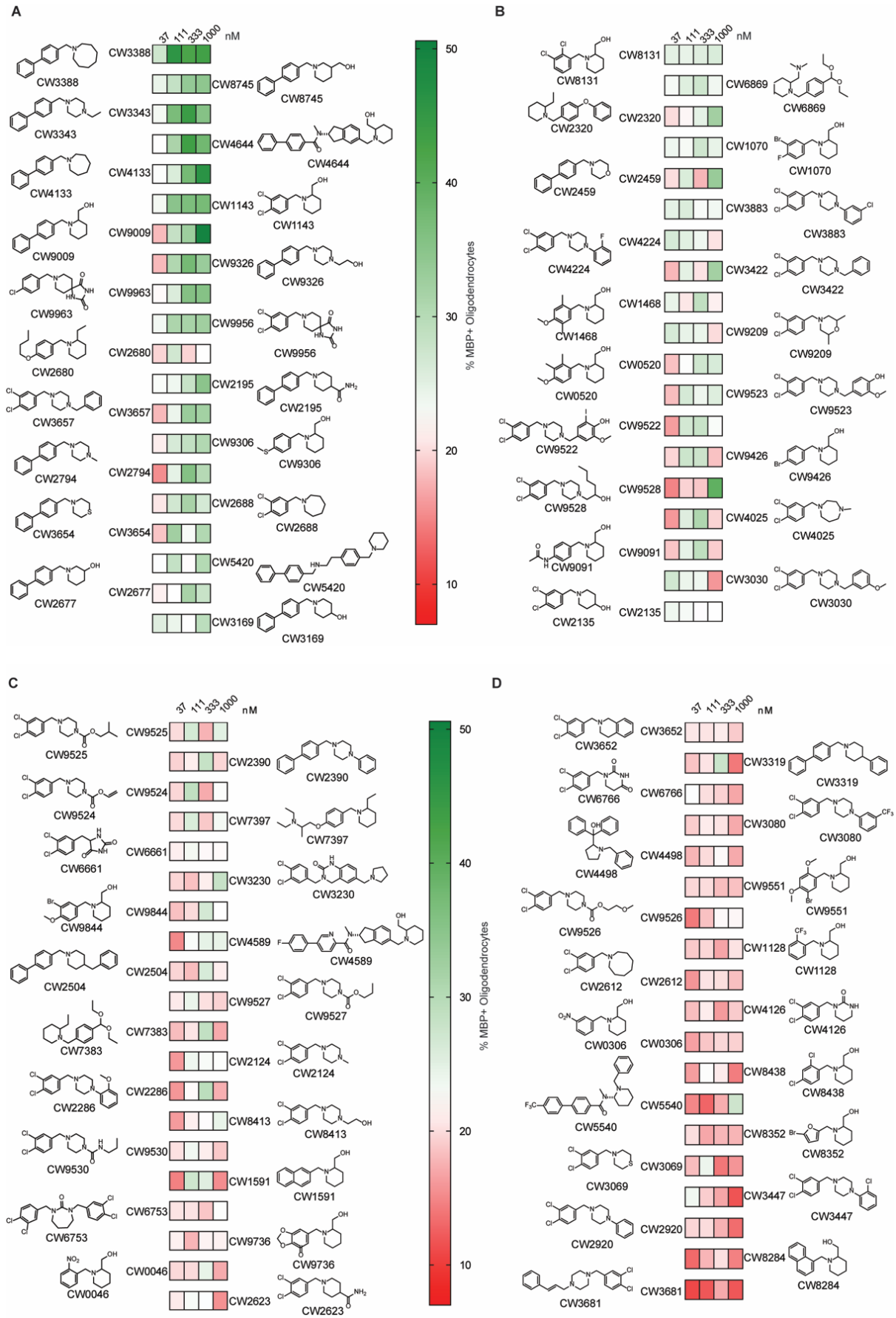

Data S2. Structures of 76 structural analogs with heat-maps representing the percentage of MBP+ oligodendrocytes generated after treatment with each small molecule for 72 h. Related to Figure 3.

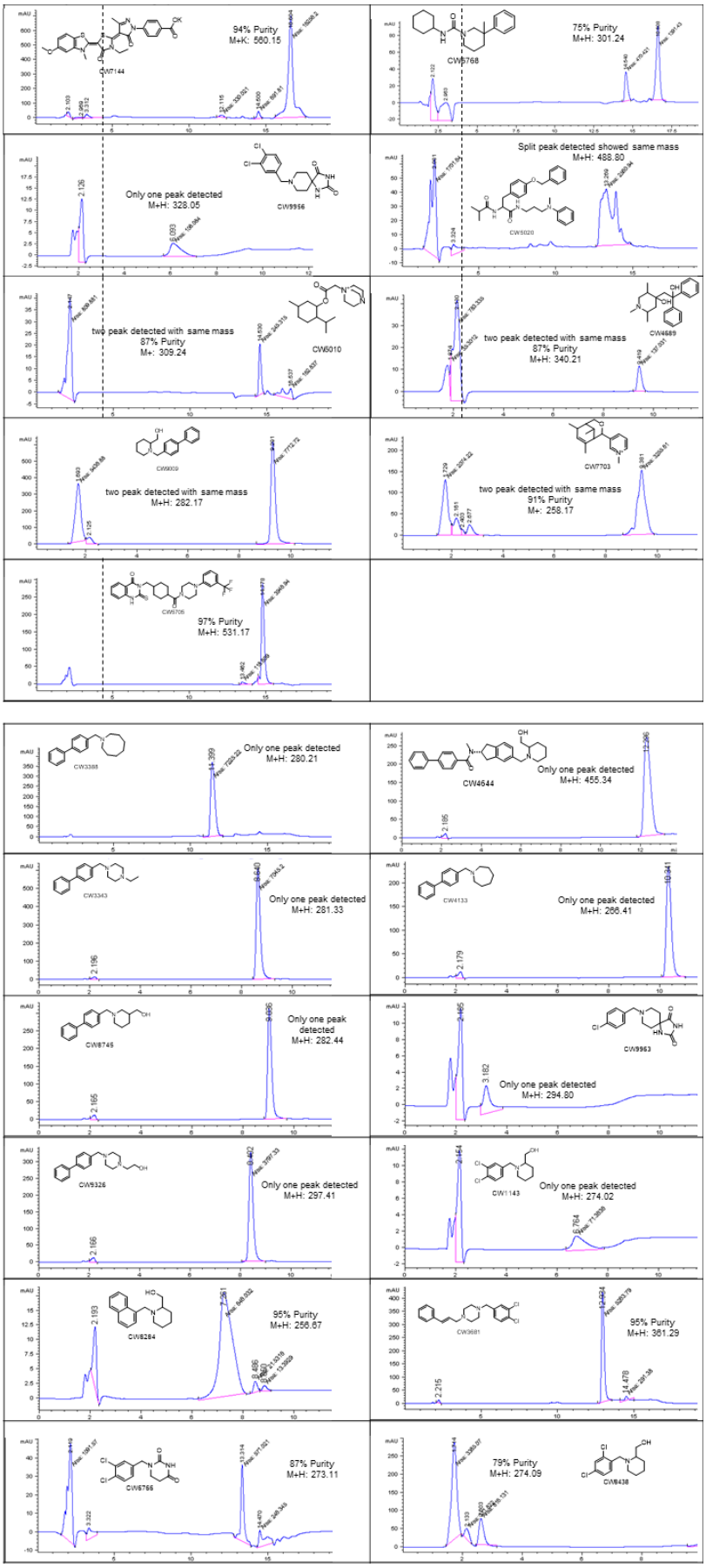

Data S3. Purity of compounds estimated using liquid chromatography-mass spectrometry (LC-MS). Related to Figure 3.